# Neodymium isotopes in peat reveal past local environmental disturbances

Katarzyna Marcisz[a]*, Zdzislaw Belka[b], Jolanta Dopieralska[c], Michał Jakubowicz[b], Monika Karpińska-Kołaczek[a], Piotr Kołaczek[a], Dmitri Mauquoy[d], Michał Słowiński[e], Mateusz Zieliński[b], Mariusz Lamentowicz[a]

[a] Climate Change Ecology Research Unit, Adam Mickiewicz University, Poznań, Poland

[b] Isotope Research Unit, Adam Mickiewicz University, Poznań, Poland

[c] Isotope Laboratory, Poznań Science and Technology Park, Adam Mickiewicz University Foundation, Poznań, Poland

[d] School of Geosciences, University of Aberdeen, Aberdeen, UK

[e] Past Landscape Dynamics Laboratory, Institute of Geography and Spatial Organization, Polish Academy of Sciences, Warsaw, Poland

*Corresponding author: marcisz@amu.edu.pl (K. Marcisz)

## Graphical abstract

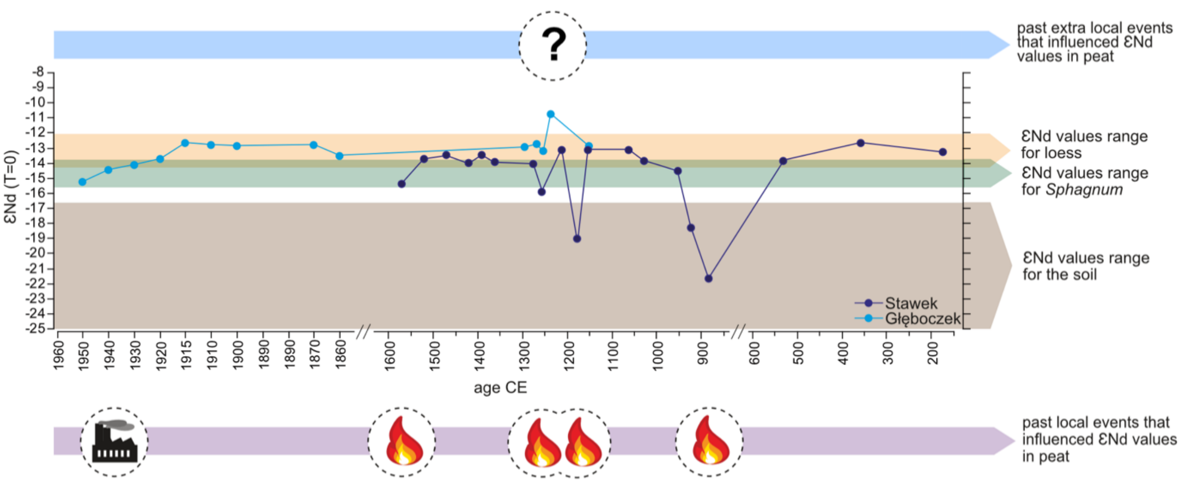

**Abstract**

Over the past decade, the neodymium (Nd) isotope composition of mineral matter from peat cores has seen increasingly common use as a tracer of dust influx associated with major changes in the Holocene atmospheric circulation. However, the incomplete understanding of the local controls on the sources of the sediment supplied to peatlands remains a key difficulty in the interpretation of the archived Nd isotope signals. Here, we used neodymium isotopes to reconstruct environmental disturbances in peatlands. We performed a multi-proxy study of two peatlands that experienced peatland burning and validated the recorded peat Nd signatures using reference surface sampling. Our data show a link between the Nd isotope signals and local environmental disturbances: peat burning, local fire activity and pollution fluxes. Our study illustrates the crucial role of identifying local events that influence the supply of mineral material to peatlands. Insufficient recognition of such local controls may either obscure the large-scale variations in the atmospheric circulation patterns, or introduce artefacts to the Holocene climate record. We also provide recommendations for the use of Nd isotopes in palaeoecological studies of peatlands.

**Keywords**: peatlands, palaeoecology, *Sphagnum*, dust deposition, high resolution, geochemistry, Poland

## 1. Introduction

Ongoing global changes and anthropogenic pressure significantly influence ecosystems worldwide (IPCC, 2022). Peatland ecosystems comprise one of essential carbon stocks in the world and are necessary for climate change mitigation (IPCC, 2019; Parish et al., 2008). Peatlands are experiencing various forms of disturbances, which include drainage and substantial drying (Holden et al., 2006; Kettridge et al., 2015; Swindles et al., 2019), peat extraction (Bravo et al., 2020; Łuców et al., 2022), and fires (Guêné-Nanchen et al., 2022; Turetsky et al., 2015; Witze, 2020). All these disturbances damage peat carbon stocks, and significantly influence global carbon and methane emissions to the atmosphere (Gallego-Sala et al., 2018). To support ecosystem restoration and predict future trajectories of peatlands' development, it is crucial to recognize how disturbances impacted peatlands in the past (Karpińska-Kołaczek et al., 2022; Marcisz et al., 2022; Słowiński et al., 2019).

A number of proxies are commonly used in palaeoecological studies to reconstruct past disturbances. In both peat and lake sediments, charcoal is widely used as a proxy for past fire activity (Tinner and Hu, 2003; Whitlock and Larsen, 2001), whereas certain pollen types (such as *Secale cereale* or Cerealia) inform about human presence in the study area (Kołaczek et al., 2021; Poska et al., 2004; Schwörer et al., 2021). Plant macrofossils, such as brown mosses, *Sphagnum* mosses, or vascular plants, bring important information about past environmental conditions, peatland trophic status, and local vegetation changes (Birks, 2013; Mauquoy and van Geel, 2013). As the water table depth is an essential indicator of peatlands' stability and ecological status, past hydrological reconstructions based on testate amoeba communities are commonly used to support palaeoecological interpretations (Mitchell et al., 2008). Finally, X-ray fluorescence spectrometry can serve to assess element input from dust deposition or pollution associated with anthropogenic disturbances (Fiałkiewicz-Kozieł et al., 2018; Gałka et al., 2019; Turner et al., 2014).

Neodymium (Nd) isotope composition of mineral material is a technique commonly applied in a broad range of geological studies (e.g., Allegre et al., 1979; Belka et al., 2021; Jakubowicz et al., 2021; Pearce et al., 2013; van de Flierdt et al., 2016; White and Hofmann, 1982). In recent years, the Nd isotope composition of mineral material from peat has emerged as a new tool used in palaeoecological studies, most notably to reconstruct atmospheric dust fluxes. Owing to the distinct Nd isotope ratios of different types of crustal materials (Goldstein and Jacobsen, 1988; Shaw and Wasserburg, 1985), Nd isotopes are commonly used in geological studies to trace sediment provenance, including the transport of airborne particles (Goldstein et al., 1984; Grousset and Biscaye, 2005). In peat, Nd isotopes have served to identify atmospheric dust deposition, mainly from distant sources, such as volcanic dust or desert particles, over the Holocene period (Allan et al., 2013; Fagel et al., 2014; Le Roux et al., 2012; Pratte et al., 2017a; Pratte et al., 2017b; Vanneste et al., 2016; Vanneste et al., 2015). These studies focused on large-scale atmospheric circulation patterns, attributing the changes in Nd isotope signals to variations in the continent-wide transport of dust particles. Another set of studies applied Nd isotopes to detect traces of anthropogenic pollution in peatlands (Fiałkiewicz-Kozieł et al., 2022; Fiałkiewicz-Kozieł et al., 2016).

In this multi-proxy study, we provide high-resolution records of Nd isotope ratios ($^{143}Nd/^{144}Nd$) from two peat cores from Northern Poland to assess to what extent Nd isotopes can be used to identify local disturbance events in peatlands. Except for the peat, our Nd isotope analyses included samples of surface *Sphagnum* and local soil, enabling the identification of the local sources of material deposition in the peatland basin. We hypothesize that local environmental changes, such as fire or deforestation can lead to increased mineral and dust input into the peatland and thus affect its Nd isotope signatures. Our results provide important new constraints on the possible role of the local environmental changes in shaping the Nd isotope record archived in peat cores. On a more general scale, this study allows a better understanding of both the potential and limitations of the dust provenance studies based on the Nd isotope composition of peat cores.

## 2. Study sites and methods

### *2.1 Location of studied sites and fieldwork*

We sampled two *Sphagnum*-dominated peatlands – Głęboczek and Stawek – located in Northern Poland in the Tuchola Pinewoods, a *Pinus sylvestris* monoculture forest (Figure 1). Both sites are small kettle holes (< 1 ha) covered by birch and pine with numerous collapsed dead trees; their vegetation is dominated by *Sphagnum* spp. The study area is close to the Pomeranian ice margin of the Vistulian Glaciation (ca. 17,000–16,000 cal. BP; Marks, 2012). The peatlands are located in a young glacial landscape dominated by glacial till, with common depressions and melting forms (Słowiński et al., 2015). The Głęboczek peatland basin is part of a larger lake and peatland cascade complex in the Czechowskie lake catchment (Lamentowicz et al., 2019; Ott et al., 2018), whereas the Stawek peatland is located in a depression formed by melting ice. The area of the Tuchola Pinewoods is characterized by a warm summer transitional climate, the coldest month being January (mean temperature for the period 1991–2021: −1.6°C) and the warmest July (mean 1991–2021 temperature: 18.7°C); the annual precipitation reaches 667 mm (Climate Data, 2022).

Peat coring in Głęboczek was done in March 2016, whereas coring in Stawek and surface sampling on both sites took place in May 2020. Both peat cores were retrieved using an Instorf corer – 1 m-long with 10 cm diameter in Głęboczek (Lamentowicz et al., 2019) and 50 cm-long with 5 cm diameter in Stawek. Peat cores were packed into plastic tubes and wrapped in plastic; *Sphagnum* from each peatlands' surface (picked by hand) and soil samples (sampled using a small shovel) were placed in string bags in the field and transported to the laboratory.

### *2.2 Laboratory work*

From each peatland, a 20 cm-long peat sequence (Głęboczek bog: 16–36 cm; Stawek bog: 90–110 cm) has been analyzed contiguously every 1 cm. We performed the following analyses: peat properties, peat carbon accumulation rates, pollen, non-pollen palynomorphs, plant macrofossils, testate amoebae, and microscopic and macroscopic charcoal. Neodymium isotope ratios were measured from the peat core, from the same depths as the other proxies. Moreover, from each site, *Sphagnum* and nearby soil were sampled from the surface to obtain reference measurements for Nd isotope analyses (Figure 1).

### *2.2.1 Radiocarbon dating and age-depth modelling*

The absolute chronology of the cores is based upon Bayesian age-depth models. The sample selection for the $^{14}C$ AMS dates comprised plant macrofossils and macro-charcoal pieces. Moreover, in the case of the Głęboczek core the topmost 28.5 cm were dated using the $^{210}Pb$ method. The age-depth model for the Głęboczek core is available in Lamentowicz et al. (2019). The age-depth model for the core from Stawek peatland is based on five $^{14}C$ AMS dates of charcoal pieces present in peat samples, resulting in five dates for a 20 cm-long profile (×1 AMS date every 5 cm; Table 1, Figure 2). This model was calculated in the OxCal software (*P_Sequence* function; Bronk Ramsey, 1995; Bronk Ramsey and Lee, 2013), applying the IntCal20 radiocarbon age calibration curve (Reimer et al., 2020).

### *2.2.2 Peat properties and carbon accumulation rates*

From the Głęboczek peatland, the material for bulk density, loss on ignition ($LOI_{550}$) and peat carbon accumulation rates (CAR) analyses was recovered from the frozen peat core using an empty drill that produced a peat pellet of a known volume, which enabled a continuous 2-cm sampling resolution (see Lamentowicz et al. (2019) for details). From the Stawek peatland, the peat was carefully cut into slices (2 $cm^3$ in volume, uncompressed, continuously every 1 cm). Each peat sample was dried, weighed, burnt at 550 °C for 12 h, and weighed again, following the protocol by Heiri et al. (2001). The accumulation rates derived from the peat-core chronology were multiplied by the ash-free bulk density measurement and multiplied by 50% to obtain CAR, following the protocol by Loisel et al. (2014).

### *2.2.3 Pollen and non-pollen palynomorphs*

A total of 40 samples (2 $cm^3$ in volume) for palynological analysis were prepared using standard laboratory procedures (Berglund and Ralska-Jasiewiczowa, 1986). Four of twenty pollen samples from the Głęboczek core were described earlier in Lamentowicz et al. (2019). Samples were treated with 10% HCl to dissolve carbonates and heated in 10% KOH to remove humic compounds. Afterwards, acetolysis was applied for 2.5 min. Pollen and selected non-pollen palynomorphs (NPPs) were counted under a biological microscope until the total pollen sum (TPS) in each sample reached at least 500. Pollen grains and NPPs were identified with the help of identification keys (Beug, 2004; Moore et al., 1991) and online databases (Shumilovskikh et al., 2022). The results of the palynological analysis are expressed as percentages, based on calculations of the ratio of an individual taxon to the TPS, i.e., the sum of arboreal pollen (AP) and non-arboreal pollen (NAP) excluding aquatic and wetland plants but including Cyperaceae.

### *2.2.4 Plant macrofossils*

The plant macrofossil composition of 40 peat samples (ca. 5 $cm^3$ in volume) was determined by wet sieving (mesh diameter: 125 μm). Plant macrofossils were analyzed using a binocular microscope and identified using a reference collection of type material (Mauquoy and van Geel, 2007; Tobolski, 2000). Volume percentages were estimated for all components, except seeds, roots, sand, cortex, wood and cones, counted and expressed as the number (n) present in each subsample. The plant macrofossil data from Głęboczek were published in Lamentowicz et al. (2019).

### *2.2.5 Testate amoebae and reconstructions of water table depth*

The testate amoeba (TA) composition was determined from 40 peat samples (ca. 5 $cm^3$ in volume). Four of twenty TA samples from the Głęboczek core were presented earlier in Lamentowicz et al. (2019). Peat samples were washed under 300 μm sieves following the method described by Booth et al. (2010). Testate amoebae were analyzed under a light microscope with a minimum of 100 tests per sample whenever possible (Payne and Mitchell, 2009). Testate amoebae were identified with the help of taxonomic monographs (Clarke, 2003; Mazei and Tsyganov, 2006; Ogden and Hedley, 1980) and online resources (Siemensma, 2022). The results of the TA analysis were used for the quantitative water table depth reconstructions. Quantitative reconstructions of the TA-based depth to the water table (DWT) were performed in C2 software (Juggins, 2003), using training sets developed for northern Poland (Głęboczek; Lamentowicz and Mitchell, 2005, Lamentowicz et al., 2008), and a European transfer function model (Stawek; Amesbury et al., 2016).

### *2.2.6 Charcoal*

Microscopic charcoal particles (> 10 µm) were counted from pollen slides until the number of charcoal particles and *Lycopodium* spores, counted together, exceeded 200 (Finsinger and Tinner, 2005). Microscopic charcoal influx/accumulation rates (MIC; particles/cm$^2$/year) were calculated by multiplying charcoal concentrations (particles/cm$^3$) by peat accumulation rates (Davis and Deevey, 1964; Tinner and Hu, 2003).

For macroscopic charcoal analysis, peat samples (1 cm$^3$ in volume) were prepared following the method described by Whitlock and Larsen (2001). Charcoal particles (> 500 µm) were counted under a stereoscopic microscope. Macroscopic charcoal influx/accumulation rates (MAC, particles/cm$^2$/year, a proxy for local fires; Adolf et al., 2018; Conedera et al., 2009) were calculated using the charcoal concentrations and the peat accumulation rates. The charcoal data from Głęboczek were published in Lamentowicz et al. (2019).

### *2.2.7 Neodymium isotope measurements*

All analytical procedures and isotopic measurements were carried out in the Isotope Laboratory of the Adam Mickiewicz University, Poznań, Poland. Peat samples as well as surface *Sphagnum* and soil samples from both peatlands were dried and burned at 550 °C overnight. Prior to preparation for isotopic measurements, the ash of peat and soil samples was dissolved on a hot plate (~100 °C for three days) in closed PFA vials using a mixture of concentrated hydrofluoric- and nitric acids (4:1). The ash of fresh plant material was digested in 16 N $HNO_3$. Miniaturized chromatographic techniques described by Pin et al. (1994) were utilized for the separation of Nd and Sr, with some modifications in column size and reagent concentrations according to Dopieralska (2003). The USGS reference material BHVO-2 was digested and analyzed during this study in order to monitor the analytical precision; it gave a value of 0.512986 ± 0.000006 (2σ; n=2) for $^{143}Nd/^{144}Nd$. Neodymium (loaded as phosphate) was measured on rhenium (Re) in a double-filament configuration. Isotopic ratios were collected in dynamic mode on a Finnigan MAT 261 multi-collector thermal ionization mass spectrometer (TIMS). Total procedural blanks were less than 40 pg and were found to be negligible for the results. Nd isotope ratios were normalized to $^{146}Nd/^{144}Nd = 0.7219$. Repeated measurements of the AMES standard yielded $^{143}Nd/^{144}Nd = 0.512120 \pm 10$ (2σ, n = 15).

Nd isotope data are reported in the standard epsilon (ε) notation (DePaolo and Wasserburg, 1976), which is the deviation in parts per ten thousand from the chondritic uniform reservoir (CHUR):

$$\varepsilon_{Nd} = 10000 \times [{}^{143}Nd/{}^{144}Nd_{sample} - {}^{143}Nd/{}^{144}Nd_{CHUR}] / {}^{143}Nd/{}^{144}Nd_{CHUR}.$$

It has been calculated using $^{143}Nd/^{144}Nd = 0.512638$ and $^{147}Sm/^{144}Nd = 0.1967$ for the present-day CHUR (Jacobsen and Wasserburg, 1980).

## 3. Results and interpretation

### *3.1 Absolute chronology*

The analyzed segment of the Stawek peat core covers ca. 1400 years of peatland development (ca. 170–1570 CE; Table 1. Figure 2). The age-depth model for this peat sequence has a high quality (very high agreement index = 94 %; cf. Bronk Ramsey, 2008) and shows consistent peat growth (no outliers among the $^{14}C$ dates). However, regularly occurring charcoal horizons point to increased fire activity and a possibility of hiatuses in the peat.

The analyzed Głęboczek peat section covers ca. 800 years of peatland development (ca. 1150–1970 CE). The high-resolution model, based on $^{210}Pb$ and $^{14}C$ dates, enabled the identification of a ca. 500 year-long hiatus at a depth of 28 cm, which covers a period of ca. 1300–1850 CE (Lamentowicz et al., 2019).

### *3.2 Biotic proxies*

Biotic proxy results from both peatlands show disturbances affecting their development and functioning. Both peatlands experienced local peat burning, and several charcoal layers are present in the peat.

In the Stawek peatland, the peat carbon accumulation rates were very low and the peat is highly decomposed, so most of the organic material could not be identified. The identified macrofossils enabled the classification of the sediment as herbaceous peat (Figure 3, SFig. 4). The peatland was surrounded by forest composed mainly of *Pinus sylvestris*, with an admixture of *Betula, Alnus, Quercus* and *Carpinus betulus* (Figure 3, SFig. 2). Some deforestation around the site was recorded in the layers between ca. 1260–1290 CE and ca. 1390–1570 CE. Three distinct charcoal layers that suggest increased local fire activity were identified at ca. 885 CE, 1185 CE and 1365 CE, i.e., before deforestation.

The Głęboczek core is dominated by *Sphagnum* (mainly by *Sphagnum medium/divinum* and *Sphagnum cuspidatum*), with an exception at a depth of 28 cm, where, below the peak of microcharcoal, we recorded a hiatus marked by a high proportion of unidentified organic matter

(Figure 3, SFig. 4). Peat carbon accumulation rates decreased significantly in the sections above the recorded hiatus. Like in Stawek, Głęboczek bog was surrounded by a mixed forest dominated by *Pinus sylvestris*, with an admixture of *Betula, Alnus, Quercus*, and *Carpinus betulus* (Figure 3, SFig. 2). The largest deforestation took place at ca. 1290 CE, 1900–1910 CE and 1940–1970 CE. Two layers with a substantial amount of macroscopic charcoal suggest two local fire episodes, in ca. 1875 CE and 1920 CE.

Both sites' hydrological conditions were very similar regarding the reconstructed water table depth and the testate amoeba community composition (Figure 3, SFig. 3). At both sites, the reconstructed water tables were low (below 30 cm). Testate amoeba communities were dominated by the small agglutinated taxa *Cryptodifflugia oviformis* and *Schoenbornia humicola*, which are common in dry and disturbed habitats (Lamentowicz and Mitchell, 2005; Schönborn, 1987). Moreover, these species compose their shell from various sources, often agglutinating mineral material from the environment into their shells; their high abundance may indicate regular mineral deposition into the studied peatlands (Marcisz et al., 2021).

### *3.3 Neodymium isotopes*

#### *3.3.1 Reference surface samples*

The Nd isotope measurements on reference surface samples from both sites document strongly unradiogenic $\varepsilon_{Nd}$ signatures, higher in the mineral matter from *Sphagnum* samples (−13.8 and −15.5) than in the soil samples taken from nearby slopes (−16.6 and −26.5; Table 2). The study area is covered with young glacial material dominated by clay and sand originating from Scandinavia, which was transported and accumulated during the last glaciation (Marks, 2012). There have been no previous Nd isotope measurements of young glacial sediments from this area of Poland; however, the $\varepsilon_{Nd}$ values from Scandinavian rocks (southern Sweden) are similar to those measured in our soil samples ($\varepsilon_{Nd}$ = −13.6 to −26.1; (Johansson et al., 2006; Mansfeld et al., 2005)). The $\varepsilon_{Nd}$ values observed in the local *Sphagnum* material overlap with those measured for Polish loess sediments (−12.2 to −14.1; M. Zieliński, unpublished data).

### 3.3.2 Peat cores

Most of the analyzed peat samples show a moderate (~1−2.5 $\varepsilon_{Nd}$ units) variability of $\varepsilon_{Nd}$ values, ranging from −12.7 to −15.3 for the Stawek peatland, and from −12.6 to −13.7 for the Głęboczek peatland (Figures 3 and 4). In several peat layers, the $\varepsilon_{Nd}$ signatures are notably lower and similar to those measured from the soil samples (Table 2, Figure 4). At Stawek, the lowest $\varepsilon_{Nd}$ values were recorded at ca. 885–920 CE (−21.6 and −18.3), ca. 1185 CE (−19.0), ca. 1265 (−15.9), and ca. 1570 CE (−15.3). In all these peat layers, an increase in the abundance of macroscopic charcoal is observed, and before the event at ca. 1185 CE, a drop in *Pinus sylvestris* pollen occurs (Figure 3). This may indicate that the peat layers with lower $\varepsilon_{Nd}$ signatures contain mineral material transported to the peatland from the nearby slopes by surface runoff and short-range aeolian deposition during disturbance events such as local fires or deforestation.

At Głęboczek, a trend toward lower $\varepsilon_{Nd}$ values, down to −15.2, can be observed between ca. 1940 and 1960 CE. These low $\varepsilon_{Nd}$ signatures coincide with a period of dynamic industrial and economic growth in the region, suggesting an anthropogenic source of the mineral material accumulated in the peatland basin.

We recorded only a single $\varepsilon_{Nd}$ value (−10.7 at ca. 1245 CE at Głęboczek) higher than the signatures of the reference (surface) material. As this isotopic signal is not connected to changes in other proxies, it may reflect atmospheric dust deposition from extra-local sources.

## 4 Discussion

### 4.1 Connections between neodymium isotope signals and biotic proxy data

Local environmental disturbance can significantly impact the functioning of a peatland, mainly disrupting its carbon storage capacity and leading to carbon or methane emissions (Harris et al., 2022; Kettridge et al., 2015; Sothe et al., 2022). In terms of the vegetation, disturbances cause a change in local plant composition (Anggi et al., 2018), which is often observed as a shift between dominant moss communities (Gałka et al., 2019; Lamentowicz et al., 2020; Sim et al., 2019), or an expansion of vascular vegetation on the peatland surface (Buttler et al., 2015; Dieleman et al., 2015; Sillasoo et al., 2011), mainly when a drying trend is observed. The microbial food web is also significantly affected by disturbances, a pattern that has been observed in ecological (Jassey et al., 2013; Mitchell et al., 2003; Reczuga et al., 2018; Turner and Swindles, 2012) and palaeoecological studies (Lamentowicz et al., 2019; Marcisz et al., 2021; van Bellen et al., 2016; Zhang et al., 2020). Very often, the changes in local environmental components are an effect of significant disturbance – both natural and anthropogenic – and are seen in peat cores as shifts in dominant proxies present in peat layers (Dudová et al., 2012; Feurdean et al., 2017; Kołaczek et al., 2018; Sillasoo et al., 2011; Stivrins et al., 2014).

The recorded response of biological proxies and the Nd isotope measurements indicate that changes in $\varepsilon_{Nd}$ values along the peat core were mainly related to local environmental changes and disturbances recorded at the investigated sites (Figures 3 and 4). At Stawek, all of the peat samples with the lowest $\varepsilon_{Nd}$ values show significant enrichment in charcoal. A high number of charcoal pieces indicates local fire activity that could have led to substantial changes in the peatland catchment. Fires could have resulted in forest removal, and thus an increased runoff into the peatland basin. The pollen record confirms deforestation for at least two charcoal layers dated to ca. 1185–1265 CE (Figure 3). The Stawek peatland is a kettle hole mire surrounded by a ridge made of young glacial sediments, mainly moraine clay and sand (Figure 1). After deforestations, the sedimentary material derived from the slopes, with its strongly unradiogenic

Nd isotope composition, could have been washed or blown onto the peatland surface, leading to increased contribution of the local mineral matter to the observed $\varepsilon_{Nd}$ values. Our macroscopic charcoal record from Stawek suggests that at least several local fire events in the past were sufficiently large to significantly impact the peatland basin and local vegetation.

In the most recent layers of the Głęboczek sequence, dated to ca. 1915–1950 CE, we recorded a consistent drop in $\varepsilon_{Nd}$ signatures (from −12.6 to −15.2) in the time interval coinciding with a single local fire event that was followed by deforestation and an opening of the landscape (Figure 3). The $\varepsilon_{Nd}$ values drop slightly, but do not reach the values recorded in the Stawek profile. The change in $\varepsilon_{Nd}$ signatures could be an effect of anthropogenic deforestation. Still, it could also be connected to dust deposition from industrial sources in the region, as Głęboczek is located close to a few cities (23 km from Starogard Gdański, 45 km from Tczew, and 60 km from Gdańsk) whose economies have grown in the 20$^{th}$ century. The main branches of local industries were related to shipbuilding and marine transportation. Industrial sources in Western and Central Europe have been shown to display variable $\varepsilon_{Nd}$ signatures, from −9.7 to −17.5 (Lahd Geagea et al., 2008), with the lowest signals typical of heavy industry (e.g., steel plants). It is impossible to directly link the $\varepsilon_{Nd}$ signatures from the considered peat layers to industrial dust fluxes from certain locations in this area, as no such Nd isotope data are available for this part of Poland. However, this change in the Nd isotope composition could be an effect of both a local change in vegetation and fire activity, and an increasing industrial dust influx.

The only event that can be linked to atmospheric dust deposition mainly from distant sources was recorded in the Głęboczek peat dated to ca. 1245–1265 CE, in which we observed the highest $\varepsilon_{Nd}$ value. This signature is higher than the range measured for Polish loess sediments and our reference surface samples (Figure 4, Table 2). Unequivocal identification of the source of this $^{143}$Nd-enriched material is difficult. One possible source of dust that could explain the Nd isotope composition of the concerned peat layer ($\varepsilon_{Nd}$ = −10.7) is Saharan dust, in which $\varepsilon_{Nd}$

values range from −10.0 to −15.0 (Abouchami et al., 1999; Grousset and Biscaye, 2005); a similar range of $\varepsilon_{Nd}$ signatures, attributed to an influx of Saharan dust, have been observed in older peat from Europe (Le Roux et al., 2012). However, Clifford et al. (2019), who, based on the Colle Gnifetti ice core (Swiss-Italian Alps), reconstructed Saharan dust fluxes that reached Europe over the last 2000 years, recorded such an event at 1320–1370 CE – more than half a century later than the dust flux event observed in our peat record. Given the age difference between our record and Colle Gnifetti, as well as the wide range of the Saharan dust $\varepsilon_{Nd}$ signatures, covering the entire set of our local signatures (Figure 4), it is impossible to detect Saharan dust using Nd isotopes alone. Another possible source of dust in this layer could be a volcanic eruption recorded in the mid-13$^{th}$ century. Volcanic-derived materials typically show strongly radiogenic, positive $\varepsilon_{Nd}$ values (e.g., Goldstein and Jacobsen, 1988; Shaw and Wasserburg, 1985). Icelandic volcanic ash ($\varepsilon_{Nd}$ = +5 to +10; Cohen and O'Nions, 1982; Farmer et al., 2003; Grousset et al., 1993), which often reaches continental Europe, has been present in peat sediments throughout the Holocene in many European locations (Watson et al., 2016), including peatlands in northern Poland (Watson et al., 2017). Two mid-13$^{th}$ century eruptions of the Katla volcano, dated to 1245 CE and 1262 CE (Larsen, 2000), could have been a source of the $^{143}$Nd-enriched material in this peat layer. A suitable candidate could also be a massive volcanic eruption dated to 1257 CE or 1258 CE (Emile-Geay et al., 2008; Oppenheimer, 2003), which happened in south-east Asia, possibly from the Samalas volcano located on Lombok Island in Indonesia (Lavigne et al., 2013). In the absence of additional evidence, such as the identification of volcanic tephra in the analyzed core, the exact origin of the atmospheric ash for the concerned interval cannot be identified with certainty; we can only imply an extra-local source of this dust influx.

### *4.2 Detection of local environmental disturbances and identification of local sediment sources using neodymium isotopes*

Our study aimed to assess to what extent neodymium isotopes can archive local disturbance events. Therefore, it is essential to estimate the reference $\varepsilon_{Nd}$ values of the dominant sources of mineral matter in the study area, based on which we can define the local and extra-local (regional to global) dust fluxes and their sources. Studies from Canadian peatlands showed that the most distinct changes in $\varepsilon_{Nd}$ values are related to the type of peat investigated (Pratte et al., 2017a; Pratte et al., 2017b). In these studies, minerotrophic (fen) peat sequences yielded $\varepsilon_{Nd}$ values between −29.0 and −36.0 (Pratte et al., 2017b) and between −17.0 and −21.0 (Pratte et al., 2017a). For ombrotrophic sections of the analyzed sequences, the $\varepsilon_{Nd}$ signatures ranged from −12.0 to −20.0 (mean ≈ −13.0) in a peat bog in western Quebec (Pratte et al., 2017b), as well as from −11.8 to −13.1 and from −12.6 to −15.0 in peatlands in south-eastern Quebec (Pratte et al., 2017a). Studies from Belgium showed an even smaller variability of $\varepsilon_{Nd}$ values, ranging from −10.0 to −13.0 (Fagel et al., 2014) and from −5.0 to −13.0 (Allan et al., 2013). The ombrotrophic sections gave $\varepsilon_{Nd}$ values between −10.0 and −13.0 (Fagel et al., 2014), whereas the minerotrophic sections: between −5.0 and −9.0 (Allan et al., 2013). A similar range of signatures in most of the peat samples (−7.5 to −12.5, with a single outlier having $\varepsilon_{Nd} = -1.0$) have been noted by Le Roux et al. (2012) from a Swiss peatland. The range of $\varepsilon_{Nd}$ values of the mineral matter from our peat and surface *Sphagnum* samples (Table 2, Figure 4) is similar to those from the ombrotrophic peat sections in Canada and Belgium. Both peat sections that we investigated represent ombrotrophic, *Sphagnum*-dominated peatlands, and thus show moderate variability in their Nd isotope signatures. Based on the comparison between previous research results and our reference measurements, the $\varepsilon_{Nd}$ values of the dominant, background dust flux in Poland most likely ranges from −12.0 to −15.0, and are similar to other European locations and those in Canada. Therefore, any excursions in the $\varepsilon_{Nd}$ record that are notably below or above this range likely reflect significant environmental changes in the peatland area. Moreover, due to the location of the studied peatlands in the young-glacial area, the sedimentary material on which the peatlands formed represents a mixture of various Scandinavian rocks (Marks et al., 2016), which possess a high variability of $\varepsilon_{Nd}$ signatures – from −24.7 to +2.9 (Andersen et al., 2001; Andersson et al., 2007; Johansson et al., 2016; Kara et al., 2018; Mansfeld et al., 2005).

Interpretations regarding local dust or mineral sources in peat have been mentioned in some of the previously published Nd isotope studies. However, these studies did not include reference samples collected in close proximity to the peatlands, and they refer solely to $\varepsilon_{Nd}$ data from the literature, measured at locations distant from the investigated sites (Allan et al., 2013; Fagel et al., 2014; Le Roux et al., 2012). Moreover, the authors did not define what they mean by a "local source", and how far from the site this local source may be located. For example, Le Roux et al. (2012) attributed the observed variability in the $\varepsilon_{Nd}$ values to shifts between a local source and Saharan dust, but, in the absence of additional data, provided no unequivocal evidence for the contribution of the latter. As illustrated by the present study, reference sampling from known sources of mineral material is vital to properly assess the range of the $\varepsilon_{Nd}$ values available in the proximity of a study site, and thus to enable differentiation between the signals from local *vs* extra-local sediment sources. In Patagonia, for example, a wide set of local Nd isotope data (Gaiero et al., 2007) made it possible to define local sources of dust, such as morainic material or outwash deposits (Vanneste et al., 2016; Vanneste et al., 2015). Accordingly, a good knowledge of local geology, geomorphology and hydrology is necessary, to cover the highest possible range of input sources. This is especially important when no reference measurements are available from investigated areas – which is the case for many locations.

### *4.3 Detection of distant dust fluxes*

The transport of dust particles is controlled by atmospheric conditions in a given area and dominant air masses that transport dust produced by different source regions or ecosystems. One of the main distant (extra-local) sources that can reach European peatlands is Saharan dust.

It is most often observed in the Mediterranean region, but it has reached distant European locations (including UK or Scandinavia) many times in the past (Ansmann et al., 2003; Clifford et al., 2019; Varga, 2020). The transport of Saharan dust to Europe is associated with climate change resulting in the aridification of the Sahara and is connected with the cyclone activity inside and around the Sahara (Papayannis et al., 2008). Therefore, many palaeoecological studies in Europe directed towards the identification of potential drought periods linked some shifts in the $\varepsilon_{Nd}$ values with Saharan dust influx (Allan et al., 2013; Fagel et al., 2014; Le Roux et al., 2012). Le Roux et al. (2012) interpreted the low $\varepsilon_{Nd}$ values recorded in a Swiss peatland, falling between −12.5 and −15.0, as a signal of Saharan dust; similarly, Allan et al. (2013) and Fagel et al. (2014) attributed the $\varepsilon_{Nd}$ values of Belgian peatlands, ranging from −11.0 to −12.0 and from −12.5 to −13.5, respectively, to the influx of Saharan aerosols. The range of $\varepsilon_{Nd}$ values measured for Saharan dust falls between −11.0 and −15.0 (Abouchami et al., 1999; Grousset and Biscaye, 2005). These signatures overlap with the range of $\varepsilon_{Nd}$ values measured for the mineral matter from peat and surface *Sphagnum* samples in this study (−12.6 to −15.5) and peat from other European peatlands (−10.0 to −15.0; Allan et al., 2013; Fagel et al., 2014; Le Roux et al., 2012), and thus with the general (background) dust flux present in Europe (Lahd Geagea et al., 2008). A comparison of these records shows that it is practically impossible to identify Saharan dust supply to a peatland based only on Nd isotopes alone; other, supporting evidence is needed to unequivocally detect Saharan-derived materials. The apparent coincidence of a change in the $\varepsilon_{Nd}$ values and a reconstructed age of a specific peat layer is not direct evidence, as age-depth models are often not precise enough to allow such direct comparisons (Trachsel and Telford, 2016).

Another common source of distant ash influx are volcanic eruptions, where ashes – under suitable conditions – can be transported to very distant locations, reaching other continents (Cashman and Rust, 2020; Stevenson et al., 2015). Volcanic layers have been identified using

Nd isotopes in peatlands in Europe (Allan et al., 2013; Le Roux et al., 2012) and in Patagonia (Vanneste et al., 2016; Vanneste et al., 2015). Identification of the European volcanic influx may be difficult based on Nd isotope data alone, as there are no Nd isotope measurements available for European (Iceland, the Massif Central or Laacher See) volcanic tephras. Le Roux et al. (2012) attributed their Nd isotope record ($\varepsilon_{Nd}$ values of −9.7 and −9.6) to a supply of the Icelandic Vedde Ash, but this interpretation was supported only by the age of the peat layer in which the change in the $\varepsilon_{Nd}$ values occurred. Similarly, the highest measured $\varepsilon_{Nd}$ value of −1.0 was assigned to two eruptions from the Massif Central, because of the similar age of this peat layer, rather than the similarity of the $\varepsilon_{Nd}$ signatures (Le Roux et al., 2012). For a Belgian peatland, Allan et al. (2013) also linked the $\varepsilon_{Nd}$ value of −5.5 to a volcanic ash influx from Iceland. However, there is no evidence for the specifically Icelandic origin of this $^{143}$Nd-enriched material. In fact, in their interpretation, Allan et al. (2013) erroneously used the $\varepsilon_{Nd}$ and La/Yb *vs* La/Sm signatures of subduction-related, island-arc volcanics (Handley et al., 2011), rather than that of, mid-ocean ridge-related, Iceland. Moreover, the amount of volcanic ash reaching Europe is relatively low and the volcanic signal may be too weak to dominate the local Nd signal. In contrast, studies from Patagonia, where tephra layers are often notable visually, were able to record tephra layers using the peat $\varepsilon_{Nd}$ signals, because the Nd isotope data are available for many sources from the region, including Hudson volcano dust ($\varepsilon_{Nd}$ = +2.8; Gaiero et al., 2007). Such layers have been recorded in two peatlands in Patagonia (Vanneste et al., 2016; Vanneste et al., 2015). The $\varepsilon_{Nd}$ values observed in these peatlands, ranging from −1 to +2.8 (Vanneste et al., 2016) and from −3.9 to +2.6 (Vanneste et al., 2015), are different from the signatures observed in peatlands of the Northern Hemisphere.

The impact of anthropogenic activity on peatlands has constantly been rising over the last 200 years (Loisel et al., 2021; Swindles et al., 2019), and intensified in the 20$^{th}$ century (Tanneberger et al., 2021). As most of the anthropogenic dust from industrial sources in Europe shows $\varepsilon_{Nd}$

values lower than −12.0, and even lower than −15.0 for heavy industry (Lahd Geagea et al., 2008), we interpret the decrease in the $\varepsilon_{Nd}$ values observed in Głęboczek, in the first half of the 20th century, as an effect of increasing anthropogenic forcing. Publications focused on the anthropogenic impacts over the last centuries identified anthropogenic dust flux with $\varepsilon_{Nd}$ values between −6.5 and −8.0 (Fiałkiewicz-Kozieł et al., 2022; Fiałkiewicz-Kozieł et al., 2016). However, these studies explored peatlands in Western Siberia (Fiałkiewicz-Kozieł et al., 2016) and North-Eastern China (Fiałkiewicz-Kozieł et al., 2022), which have different dust sources and thus possibly different $\varepsilon_{Nd}$ values compared to European peatlands.

## 5 Conclusions and recommendations

We performed a multi-proxy palaeoecological study of two peat cores, combining biotic-proxy data with Nd isotopic analyses to reconstruct past disturbance events. Using reference sampling, we obtained detailed information about the Nd isotope composition of the local sources of mineral material available for both investigated sites. These data enabled the detection of changes in the sources of dust and mineral flux in both cores. Applying the constraints from the local $\varepsilon_{Nd}$ values, we compared the biotic proxy and Nd isotope records, identifying mineral matter inputs associated with deforestation and fire, and distinguishing local, regional, and anthropogenic dust sources.

The relationship between the fire episodes and, to a lesser degree, human activity and pronounced shifts in the $\varepsilon_{Nd}$ values documented in the studied peat cores illustrate the critical role of local controls in shaping the Nd isotope record archived in peatlands. Recognition of such a local influence, including identifying the $\varepsilon_{Nd}$ signatures of local sediments and establishing possibly the most precise age constraints, is a prerequisite to addressing more advanced research questions, such as a possible contribution of dust influx from distant sources.

As long as the background local Nd sources are not recognized, the implications of the Nd isotope data should be evaluated with caution, and cannot be used as standalone evidence for large-scale variations in atmospheric circulation patterns.

The most crucial issues regarding the use of Nd isotopes that we identified are:

1. **Commonly low sampling resolution of Nd isotope analyses**. In many cases in the past, the sampling resolution for Nd isotope analyses was lower than for other palaeoecological proxies. Therefore, the Nd isotope records possibly showed only a fraction of past environmental changes that could have been identified if high-resolution sampling was applied. Moreover, for relatively large samples, the Nd record will likely homogenize material accumulated during several deposition events. Hence, to assure better recognition of specific past events, we recommend higher sampling resolution for Nd isotope analyses.
2. **Interpretation of Nd isotope results by directly connecting the Nd record with low-resolution age-depth models to assess possible dust sources**. Direct comparison between the Nd record, biotic-proxy data and reconstructed age is difficult if peat dating is of low resolution and does not allow the identification of potential hiatuses, sediment mixing or recognition of different peat accumulation patterns. As shown by several studies, peatland age-depth modelling requires a dense set of radiocarbon and/or lead dates throughout the core (Fiałkiewicz-Kozieł et al., 2014; Kołaczek et al., 2019; Kołaczek et al., 2018). Hence, we recommend higher resolution dating of peat cores to assure the lack of hiatuses and better recognition of specific past events recorded with the associated Nd isotope record.
3. **Lack of reference sampling and assessment of local Nd pools and arbitrary selection of Nd reservoirs to compare with Nd isotope and proxy data**. Because the Nd isotope composition of local sediments has been established only for some regions

and environmental settings, there are areas for which no such background $\varepsilon_{Nd}$ data are available. Therefore, if no reference sampling from the investigated area is done, the Nd isotope records are compared with data from arbitrarily selected, commonly distant Nd reservoirs (e.g., Saharan or Mongolian dust for European records), whereas geographically closer sources are often omitted. As an effect, many suggested sources possess very broad – and largely overlapping – ranges of $\varepsilon_{Nd}$ values that are difficult to interpret unambiguously.

4. **Interpretation of local *vs* regional inputs of Nd, as well as a direct comparison of $\varepsilon_{Nd}$ signatures between the core and some potential sources while not accounting for mixing between several sources**. One limitation of most studies published to date is that they directly compare the $\varepsilon_{Nd}$ values measured in peat to the $\varepsilon_{Nd}$ signatures of potential sources (e.g., Saharan dust, distant volcanic eruptions). We recommend to primarily focus the interpretations of $\varepsilon_{Nd}$ isotope records on major trends, rather than specific $\varepsilon_{Nd}$ values. The $\varepsilon_{Nd}$ values provide information about an increased contribution of a source that is $^{143}$Nd-enriched or $^{143}$Nd-depleted, but are often not conclusive about this source – as long as they do not fall outside the range of the background reference values. In the case of significant excursions, in turn, possible local controls should be established first, and only in the absence of 'local' explanations 'extra-local' sources can be considered.

## CRediT authorship contribution statement

KM: funding acquisition, fieldwork, testate amoeba analysis, charcoal analysis, peat properties analysis, age-depth modelling, figures, writing (original draft); ZB: neodymium data interpretation, writing (review & editing); JD: neodymium measurements, writing (review & editing); MJ: neodymium data interpretation, writing (review & editing); MK-K: testate amoeba analysis, writing (review & editing); PK: pollen analysis, age-depth modelling, figures, writing (review & editing); DM: plant macrofossil analysis, writing (review & editing); MS: fieldwork, figures, writing (review & editing); MZ: fieldwork, neodymium data interpretation, writing (review & editing); ML: fieldwork, plant macrofossil analysis, age-depth modelling, writing (review & editing)


**Funding**

The Stawek profile radiocarbon dating and investigation and neodymium measurements were financed by the National Science Centre, Poland, grants no. 2019/03/X/ST10/00849 and 2020/39/D/ST10/00641. The Głęboczek profile radiocarbon dating and investigation were financed by the National Science Centre, Poland, grant no. 2015/17/B/ST10/01656.

**To appear on Author Accepted Manuscript**

This research was funded in whole or in part by National Science Centre, Poland, grants no. 2019/03/X/ST10/00849, 2020/39/D/ST10/00641 and 2015/17/B/ST10/01656.



**Data**

All data associated with this article are openly available on Mendeley Data repository under the DOI: 10.17632/rv5h96zvpb.1

## List of tables

**Table 1**. Results of radiocarbon dating of charcoal sampled from peat from Stawek bog. The radiocarbon dates were calibrated using the IntCal20 calibration curve (Reimer et al., 2020).

**Table 2**. Reference $\varepsilon_{Nd}$ values measured in surface samples taken from the studied peatlands and their surrounding (Głęboczek – Gł; Stawek – pBS).

## List of figures

**Figure 1**. Location, geological setting, and photographs of the studied peatlands. Photographs present the collection sites for surface samples included in the neodymium isotope analyses: red dots indicate the location of soil surface samples; blue dots indicate *Sphagnum* surface samples.

**Figure 2**. Age-depth models for analyzed peat cores. A: The age-depth model for the Stawek peat sequence. The purple area outlines the 95.4 % confidence interval. B: The age-depth model for the Głęboczek peat sequence with highlighted segment investigated in this study. Details of the age-depth modelling are available in Lamentowicz et al. (2019).

**Figure 3**. $\varepsilon_{Nd}$ and selected other proxy data for the Głęboczek and Stawek peatlands. Peat layers in which biotic proxy responses coincide with marked changes in the neodymium isotope signatures are highlighted in red.

**Figure 4**. Summary illustration of the neodymium isotope records (εNd values) from the Stawek and Głęboczek peatlands. The sections highlighted with colours show the ranges of εNd values for: Polish loess sediments (yellow; M. Zieliński, unpublished data), *Sphagnum* surface samples (green; this study), local soil (brown; this study) and past disturbance events (major fires and industrial activity) that potentially influenced the εNd values measured in peat.

## Supplementary material

**Supplementary Figure 1**. Palaeoecological diagrams presenting results of the analysis of peat properties, $\varepsilon_{Nd}$ measurements, and micro- and macroscopic charcoal accumulation rates for Głęboczek and Stawek peatlands.

**Supplementary Figure 2**. Percentage pollen diagrams for Głęboczek and Stawek peatlands.

**Supplementary Figure 3**. Percentage diagrams presenting testate amoebae data and testate amoeba-based depth-to-water table reconstructions for Głęboczek and Stawek peatlands.

**Supplementary Figure 4**. Plant macrofossils diagrams for Głęboczek and Stawek peatlands.

## References


Abouchami W, Galer SJG, Koschinsky A. Pb and Nd isotopes in NE Atlantic Fe–Mn crusts: Proxies for trace metal paleosources and paleocean circulation. Geochimica et Cosmochimica Acta 1999; 63: 1489-1505.

Adolf C, Wunderle S, Colombaroli D, Weber H, Gobet E, Heiri O, et al. The sedimentary and remote-sensing reflection of biomass burning in Europe. Global Ecology and Biogeography 2018; 27: 199-212.

Allan M, Le Roux G, Piotrowska N, Beghin J, Javaux E, Court-Picon M, et al. Mid- and late Holocene dust deposition in western Europe: the Misten peat bog (Hautes Fagnes – Belgium). Clim. Past 2013; 9: 2285-2298.

Allegre CJ, Ben Othman D, Polve M, Richard P. The Nd-Sr isotopic correlation in mantle materials and geodynamic consequences. Physics of the Earth and Planetary Interiors 1979; 19: 293-306.

Amesbury MJ, Swindles GT, Bobrov A, Charman DJ, Lamentowicz M, Mallon G, et al. Development of a new pan-European testate amoeba transfer function for reconstructing peatland palaeohydrology. Quaternary Science Reviews 2016; 152: 132-151.

Andersen TOM, Andresen A, Sylvester AG. Nature and distribution of deep crustal reservoirs in the southwestern part of the Baltic Shield: Evidence from Nd, Sr and Pb isotope data on late Sveconorwegian granites. Journal of the Geological Society 2001; 158: 253-267.

Andersson UB, Rutanen H, Johansson Å, Mansfeld J, Rimša A. Characterization of the Paleoproterozoic Mantle beneath the Fennoscandian Shield: Geochemistry and Isotope Geology (Nd, Sr) of ~ 1.8 Ga Mafic Plutonic Rocks from the Transscandinavian Igneous Belt in Southeast Sweden. International Geology Review 2007; 49: 587-625.

Anggi HK, Siria B, C. JT, Peter R, Asmadi S, Supiandi S, et al. Resilience of a peatland in Central Sumatra, Indonesia to past anthropogenic disturbance: Improving conservation and restoration designs using palaeoecology. Journal of Ecology 2018; 106: 2473-2490.

Ansmann A, Bösenberg J, Chaikovsky A, Comerón A, Eckhardt S, Eixmann R, et al. Long-range transport of Saharan dust to northern Europe: The 11–16 October 2001 outbreak observed with EARLINET. Journal of Geophysical Research: Atmospheres 2003; 108.
Belka Z, Dopieralska J, Jakubowicz M, Skompski S, Walczak A, Korn D, et al. Nd isotope record of ocean closure archived in limestones of the Devonian–Carboniferous carbonate platform, Greater Karatau, southern Kazakhstan. Journal of the Geological Society 2021; 178: jgs2020-077.
Berglund BE, Ralska-Jasiewiczowa M. Pollen analysis and pollen diagrams. In: Berglund BE, editor. Handbook of Holocene Palaeoecology and Palaeohydrology. John Wiley & Sons, Chichester, 1986, pp. 455-484.
Beug H-J. Leitfaden der Pollenbestimmung für Mitteleuropa und angrenzende Gebiete. München: Verlag Dr. Friedrich Pfeil, 2004.
Birks HH. Plant macrofossils introduction. In: Elias SA, Mock CJ, editors. Encyclopedia of Quaternary Science (Second Edition). Elsevier, Amsterdam, 2013, pp. 593-612.
Booth RK, Lamentowicz M, Charman DJ. Preparation and analysis of testate amoebae in peatland paleoenvironmental studies. Mires and Peat 2010; 7 (2010/11): 1-7.
Bravo TG, Brummell ME, Rochefort L, Strack M. Effects of invasion by birch on the growth of planted spruce at a post-extraction peatland. Mires and Peat 2020; 26: 9 pp.
Bronk Ramsey C. Radiocarbon calibration and analysis of stratigraphy: The OxCal program. Radiocarbon 1995; 37: 425-430.
Bronk Ramsey C. Deposition models for chronological records. Quaternary Science Reviews 2008; 27: 42-60.
Bronk Ramsey C, Lee S. Recent and Planned Developments of the Program OxCal. Radiocarbon 2013; 55: 720-730.
Buttler A, Robroek BJM, Laggoun-Défarge F, Jassey VEJ, Pochelon C, Bernard G, et al. Experimental warming interacts with soil moisture to discriminate plant responses in an ombrotrophic peatland. Journal of Vegetation Science 2015; 26: 964-974.
Cashman KV, Rust AC. Far-travelled ash in past and future eruptions: combining tephrochronology with volcanic studies. Journal of Quaternary Science 2020; 35: 11-22.
Clarke KJ. Guide to Identification of Soil Protozoa - Testate Amoebae. Ambleside, U.K.: Freshwater Biological Association, 2003.
Clifford HM, Spaulding NE, Kurbatov AV, More A, Korotkikh EV, Sneed SB, et al. A 2000 year Saharan dust event proxy record from an ice core in the European Alps. Journal of Geophysical Research: Atmospheres 2019; 124: 12882-12900.
Climate Data. www.climate-data.org. 2022, 2022.
Cohen RS, O'Nions RK. The Lead, Neodymium and Strontium Isotopic Structure of Ocean Ridge Basalts. Journal of Petrology 1982; 23: 299-324.
Conedera M, Tinner W, Neff C, Meurer M, Dickens AF, Krebs P. Reconstructing past fire regimes: methods, applications, and relevance to fire management and conservation. Quaternary Science Reviews 2009; 28: 555-576.
Davis MB, Deevey ES. Pollen Accumulation Rates: Estimates from Late-Glacial Sediment of Rogers Lake. Science 1964; 145: 1293-1295.
DePaolo DJ, Wasserburg GJ. Nd isotopic variations and petrogenetic models. Geophysical Research Letters 1976; 3: 249-252.
Dieleman CM, Branfireun BA, McLaughlin J, Lindo Z. Climate change drives a shift in peatland ecosystem plant community: Implications for ecosystem function and stability. Glob Chang Biol 2015; 21: 388-395.
Dopieralska J. Neodymium isotopic composition of conodonts as a palaeoceanographic proxy in the Variscan oceanic system. PhD thesis. Justus-Liebig-Univ., Giessen., 2003.
Dudová L, Hájková P, Buchtová H, Opravilová V. Formation, succession and landscape history of Central-European summit raised bogs: A multiproxy study from the Hrubý Jeseník Mountains. The Holocene 2012; 23: 230-242.

Emile-Geay J, Seager R, Cane MA, Cook ER, Haug GH. Volcanoes and ENSO over the Past Millennium. Journal of Climate 2008; 21: 3134-3148.

Fagel N, Allan M, Le Roux G, Mattielli N, Piotrowska N, Sikorski J. Deciphering human–climate interactions in an ombrotrophic peat record: REE, Nd and Pb isotope signatures of dust supplies over the last 2500years (Misten bog, Belgium). Geochimica et Cosmochimica Acta 2014; 135: 288-306.

Farmer GL, Barber D, Andrews J. Provenance of Late Quaternary ice-proximal sediments in the North Atlantic: Nd, Sr and Pb isotopic evidence. Earth and Planetary Science Letters 2003; 209: 227-243.

Feurdean A, Florescu G, Vannière B, Tantau I, O'Hara RB, Pfeiffer M, et al. Fire has been an important driver of forest dynamics in the Carpathian Mountains during the Holocene. Forest Ecology and Management 2017; 389: 15-26.

Fiałkiewicz-Kozieł B, Bao K, Smieja-Król B. Geographical drivers of geochemical and mineralogical evolution of Motianling peatland (Northeast China) exposed to different sources of rare earth elements and Pb, Nd, and Sr isotopes. Science of The Total Environment 2022; 807: 150481.

Fiałkiewicz-Kozieł B, De Vleeschouwer F, Mattielli N, Fagel N, Palowski B, Pazdur A, et al. Record of Anthropocene pollution sources of lead in disturbed peatlands from Southern Poland. Atmospheric Environment 2018; 179: 61-68.

Fiałkiewicz-Kozieł B, Kołaczek P, Piotrowska N, Michczyński A, Łokas E, Wachniew P, et al. High-resolution age-depth model of a peat bog in Poland as an important basis for paleoenvironmental studies. Radiocarbon 2014; 56: 109-125.

Fiałkiewicz-Kozieł B, Smieja-Król B, Frontasyeva M, Słowiński M, Marcisz K, Lapshina E, et al. Anthropogenic- and natural sources of dust in peatland during the Anthropocene. Scientific Reports 2016; 6: 38731.

Finsinger W, Tinner W. Minimum count sums for charcoal-concentration estimates in pollen slides: accuracy and potential errors. The Holocene 2005; 15: 293-297.

Gaiero DM, Brunet F, Probst J-L, Depetris PJ. A uniform isotopic and chemical signature of dust exported from Patagonia: Rock sources and occurrence in southern environments. Chemical Geology 2007; 238: 107-120.

Gallego-Sala AV, Charman DJ, Brewer S, Page SE, Prentice IC, Friedlingstein P, et al. Latitudinal limits to the predicted increase of the peatland carbon sink with warming. Nature Climate Change 2018; 8: 907–913.

Gałka M, Szal M, Broder T, Loisel J, Knorr K-H. Peatbog resilience to pollution and climate change over the past 2700 years in the Harz Mountains, Germany. Ecological Indicators 2019; 97: 183-193.

Goldstein SJ, Jacobsen SB. Nd and Sr isotopic systematics of river water suspended material: implications for crustal evolution. Earth and Planetary Science Letters 1988; 87: 249-265.

Goldstein SL, O'Nions RK, Hamilton PJ. A Sm-Nd isotopic study of atmospheric dusts and particulates from major river systems. Earth and Planetary Science Letters 1984; 70: 221-236.

Grousset FE, Biscaye PE. Tracing dust sources and transport patterns using Sr, Nd and Pb isotopes. Chemical Geology 2005; 222: 149-167.

Grousset FE, Labeyrie L, Sinko JA, Cremer M, Bond G, Duprat J, et al. Patterns of Ice-Rafted Detritus in the Glacial North Atlantic (40–55°N). Paleoceanography 1993; 8: 175-192.

Guêné-Nanchen M, LeBlanc M-C, Rochefort L. Post-fire peatland vegetation recovery: a case study in open rich fens of the Canadian boreal forest. Botany 2022; 0: 1-13.

Handley HK, Turner S, Macpherson CG, Gertisser R, Davidson JP. Hf–Nd isotope and trace element constraints on subduction inputs at island arcs: Limitations of Hf anomalies as sediment input indicators. Earth and Planetary Science Letters 2011; 304: 212-223.

Harris LI, Richardson K, Bona KA, Davidson SJ, Finkelstein SA, Garneau M, et al. The essential carbon service provided by northern peatlands. Frontiers in Ecology and the Environment 2022; 20: 222-230.

Heiri O, Lotter AF, Lemcke G. Loss on ignition as a method for estimating organic and carbonate content in sediments: Reproducibility and comparability of results. Journal Of Paleolimnology 2001; 25: 101-110.
Holden J, Evans MG, Burt TP, Horton M. Impact of Land Drainage on Peatland Hydrology. Journal of Environmental Quality 2006; 35: 1764-1778.
IPCC. IPCC special report on climate change, desertification, land degradation, sustainable land management, food security, and greenhouse gas fluxes in terrestrial ecosystems, 2019.
IPCC. Impacts, Adaptation, and Vulnerability. Contribution of Working Group II to the Sixth Assessment Report of the Intergovernmental Panel on Climate Change. In: Pörtner H-O, Roberts DC, Tignor M, Poloczanska ES, Mintenbeck K, Alegría A, et al., editors, Cambridge University Press., 2022.
Jacobsen SB, Wasserburg GJ. Sm-Nd isotopic evolution of chondrites. Earth and Planetary Science Letters 1980; 50: 139-155.
Jakubowicz M, Agirrezabala LM, Dopieralska J, Siepak M, Kaim A, Belka Z. The role of magmatism in hydrocarbon generation in sedimented rifts: A Nd isotope perspective from mid-Cretaceous methane-seep deposits of the Basque-Cantabrian Basin, Spain. Geochimica et Cosmochimica Acta 2021; 303: 223-248.
Jassey VEJ, Chiapusio G, Binet P, Buttler A, Laggoun-Defarge F, Delarue F, et al. Above- and belowground linkages in Sphagnum peatland: climate warming affects plant-microbial interactions. Global Change Biol 2013; 19: 811-823.
Johansson Å, Bogdanova S, Čečys A. A revised geochronology for the Blekinge Province, southern Sweden. GFF 2006; 128: 287-302.
Johansson Å, Waight T, Andersen T, Simonsen SL. Geochemistry and petrogenesis of Mesoproterozoic A-type granitoids from the Danish island of Bornholm, southern Fennoscandia. Lithos 2016; 244: 94-108.
Juggins S. C2 User Guide. Software for Ecological and Palaeoecological Data Analysis and Visualisation. University of Newcastle, Newcastle upon Tyne, UK, 2003.
Kara J, Väisänen M, Johansson Å, Lahaye Y, O'Brien H, Eklund O. 1.90-1.88Ga arc magmatism of central Fennoscandia: geochemistry, U-Pb geochronology, Sm-Nd and Lu-Hf isotope systematics of plutonic-volcanic rocks from southern Finland. Geologica Acta 2018; 16: 1-23.
Karpińska-Kołaczek M, Kołaczek P, Czerwiński S, Gałka M, Guzowski P, Lamentowicz M. Anthropocene history of rich fen acidification in W Poland — Causes and indicators of change. Science of The Total Environment 2022; 838: 155785.
Kettridge N, Turetsky MR, Sherwood JH, Thompson DK, Miller CA, Benscoter BW, et al. Moderate drop in water table increases peatland vulnerability to post-fire regime shift. Scientific Reports 2015; 5: 8063.
Kołaczek P, Buczek K, Margielewski W, Gałka M, Rycerz A, Woszczyk M, et al. Development and degradation of a submontane forest in the Beskid Wyspowy Mountains (Polish Western Carpathians) during the Holocene. The Holocene 2021; 31: 1716-1732.
Kołaczek P, Gałka M, Lamentowicz M, Marcisz K, Kajukało-Drygalska K, Karpińska-Kołaczek M. Increased radiocarbon dating resolution of ombrotrophic peat profiles reveals periods of disturbance which were previously undetected. Quaternary Geochronology 2019; 52: 21-28.
Kołaczek P, Karpińska-Kołaczek M, Marcisz K, Gałka M, Lamentowicz M. Palaeohydrology and the human impact on one of the largest raised bogs complex in the Western Carpathians (Central Europe) during the last two millennia. The Holocene 2018; 28: 595-608.
Lahd Geagea M, Stille P, Gauthier-Lafaye F, Millet M. Tracing of Industrial Aerosol Sources in an Urban Environment Using Pb, Sr, and Nd Isotopes. Environmental Science & Technology 2008; 42: 692-698.
Lamentowicz Ł, Lamentowicz M, Gąbka M. Testate amoebae ecology and local transfer function from a peatland in Western Poland. Wetlands 2008; 28: 164-175.
Lamentowicz M, Kołaczek P, Mauquoy D, Kittel P, Łokas E, Słowiński M, et al. Always on the tipping point – A search for signals of past societies and related peatland ecosystem critical

transitions during the last 6500 years in N Poland. Quaternary Science Reviews 2019; 225: 105954.
Lamentowicz M, Marcisz K, Guzowski P, Gałka M, Diaconu A-C, Kołaczek P. How Joannites' economy eradicated primeval forest and created anthroecosystems in medieval Central Europe. Scientific Reports 2020; 10: 18775.
Lamentowicz M, Mitchell EAD. The ecology of testate amoebae (Protists) in Sphagnum in north-western Poland in relation to peatland ecology. Microbial Ecology 2005; 50: 48-63.
Larsen G. Holocene eruptions within the Katla volcanic system, South Iceland; characteristics and environmental impact. Jökull 2000; 49: 1.
Lavigne F, Degeai J-P, Komorowski J-C, Guillet S, Robert V, Lahitte P, et al. Source of the great A.D. 1257 mystery eruption unveiled, Samalas volcano, Rinjani Volcanic Complex, Indonesia. Proceedings of the National Academy of Sciences 2013; 110: 16742-16747.
Le Roux G, Fagel N, De Vleeschouwer F, Krachler M, Debaille V, Stille P, et al. Volcano- and climate-driven changes in atmospheric dust sources and fluxes since the Late Glacial in Central Europe. Geology 2012; 40: 335-338.
Loisel J, Gallego-Sala AV, Amesbury MJ, Magnan G, Anshari G, Beilman DW, et al. Expert assessment of future vulnerability of the global peatland carbon sink. Nature Climate Change 2021; 11: 70-77.
Loisel J, Yu Z, Beilman DW, Camill P, Alm J, Amesbury MJ, et al. A database and synthesis of northern peatland soil properties and Holocene carbon and nitrogen accumulation. The Holocene 2014; 24: 1028-1042.
Łuców D, Küttim M, Słowiński M, Kołaczek P, Karpińska-Kołaczek M, Küttim L, et al. Searching for an ecological baseline: Long-term ecology of a post-extraction restored bog in Northern Estonia. Quaternary International 2022; 607: 65-78.
Mansfeld J, Beunk FF, Barling J. 1.83—1.82 Ga formation of a juvenile volcanic arc—implications from U—Pb and Sm—Nd analyses of the Oskarshamn-Jönköping Belt, southeastern Sweden. GFF 2005; 127: 149-157.
Marcisz K, Buczek K, Gałka M, Margielewski W, Mulot M, Kołaczek P. Past testate amoeba communities in landslide mountain fens (Polish Carpathians): The relationship between shell types and sediment. The Holocene 2021; 31: 954-965.
Marcisz K, Czerwiński S, Lamentowicz M, Łuców D, Słowiński M. How paleoecology can support peatland restoration. Past Global Changes Magazine 2022; 30: 12-13.
Marks L. Timing of the Late Vistulian (Weichselian) glacial phases in Poland. Quaternary Science Reviews 2012; 44: 81-88.
Marks L, Dzierżek J, Janiszewski R, Kaczorowski J, Lindner L, Majecka A, et al. Quaternary stratigraphy and palaeogeography of Poland. Acta geologica Polonica 2016; 66: 403-427.
Mauquoy D, van Geel B. Mire and peat macrofossils, Encyclopedia of Quaternary Science. Elsevier, Amsterdam, 2007.
Mauquoy D, van Geel B. PLANT MACROFOSSIL METHODS AND STUDIES | Mire and Peat Macros. In: Elias SA, Mock CJ, editors. Encyclopedia of Quaternary Science (Second Edition). Elsevier, Amsterdam, 2013, pp. 637-656.
Mazei Y, Tsyganov AN. Freshwater testate amoebae. Moscow: KMK, 2006.
Mitchell EAD, Charman DJ, Warner BG. Testate amoebae analysis in ecological and paleoecological studies of wetlands: past, present and future. Biodiversity and Conservation 2008; 17: 2115-2137.
Mitchell EAD, Gilbert D, Buttler A, Amblard C, Grosvernier P, Gobat J-M. Structure of microbial communities in *Sphagnum* peatlands and effect of atmospheric carbon dioxide enrichment. Microbial Ecology 2003; 46: 187-199.
Moore PD, Webb JA, Collinson ME. Pollen Analysis: Blackwell Scientific Publications, Oxford, 1991.
Ogden CG, Hedley RH. An Atlas of Freshwater Testate Amoebae. London: Oxford University Press, 1980.

Oppenheimer C. Ice core and palaeoclimatic evidence for the timing and nature of the great mid-13th century volcanic eruption. International Journal of Climatology: A Journal of the Royal Meteorological Society 2003; 23: 417-426.

Ott F, Kramkowski M, Wulf S, Plessen B, Serb J, Tjallingii R, et al. Site-specific sediment responses to climate change during the last 140 years in three varved lakes in Northern Poland. The Holocene 2018; 28: 464-477.

Papayannis A, Amiridis V, Mona L, Tsaknakis G, Balis D, Bösenberg J, et al. Systematic lidar observations of Saharan dust over Europe in the frame of EARLINET (2000–2002). Journal of Geophysical Research: Atmospheres 2008; 113.

Parish F, Sirin A, Charman DJ, Joosten H, Minayeva T, Silvius M, et al. Assessment on peatlands, biodiversity and climate change: main report, 2008.

Payne RJ, Mitchell EAD. How many is enough? Determining optimal count totals for ecological and palaeoecological studies of testate amoebae. J. Paleolimnol. 2009; 42: 483-495.

Pearce CR, Jones MT, Oelkers EH, Pradoux C, Jeandel C. The effect of particulate dissolution on the neodymium (Nd) isotope and Rare Earth Element (REE) composition of seawater. Earth and Planetary Science Letters 2013; 369-370: 138-147.

Pin C, Briot D, Bassin C, Poitrasson F. Concomitant separation of strontium and samarium-neodymium for isotopic analysis in silicate samples, based on specific extraction chromatography. Analytica Chimica Acta 1994; 298: 209-217.

Poska A, Saarse L, Veski S. Reflections of pre- and early-agrarian human impact in the pollen diagrams of Estonia. Palaeogeography Palaeoclimatology Palaeoecology 2004; 209: 37-50.

Pratte S, De Vleeschouwer F, Garneau M. Geochemical characterization (REE, Nd and Pb isotopes) of atmospheric mineral dust deposited in two maritime peat bogs from the St. Lawrence North Shore (eastern Canada). Journal of Quaternary Science 2017a; 32: 617-627.

Pratte S, Garneau M, De Vleeschouwer F. Increased atmospheric dust deposition during the Neoglacial in a boreal peat bog from north-eastern Canada. Palaeogeography, Palaeoclimatology, Palaeoecology 2017b; 469: 34-46.

Reczuga MK, Lamentowicz M, Mulot M, Mitchell EAD, Buttler A, Chojnicki B, et al. Predator–prey mass ratio drives microbial activity under dry conditions in Sphagnum peatlands. Ecology and Evolution 2018; 8: 5752-5764.

Reimer PJ, Austin WEN, Bard E, Bayliss A, Blackwell PG, Bronk Ramsey C, et al. The IntCal20 Northern Hemisphere Radiocarbon Age Calibration Curve (0–55 cal kBP). Radiocarbon 2020; 62: 725-757.

Schönborn W, Petz, W., Wanner, M., and Foissner, W. Observations on the Morphology and Ecology of the Soil-Inhabiting Testate Amoebae *Schoenbornia humicola* (SCHÖNBORN, 1964) DECLOITRE, 1964 (Protozoa, Rhizopoda). Archiv für Protistenkunde 1987; 134: 315-330.

Schwörer C, Gobet E, van Leeuwen JFN, Bögli S, Imboden R, van der Knaap WO, et al. Holocene vegetation, fire and land use dynamics at Lake Svityaz, an agriculturally marginal site in northwestern Ukraine. Vegetation History and Archaeobotany 2021; 31: 155-170.

Shaw HF, Wasserburg GJ. Sm-Nd in marine carbonates and phosphates: Implications for Nd isotopes in seawater and crustal ages. Geochimica et Cosmochimica Acta 1985; 49: 503-518.

Shumilovskikh LS, Shumilovskikh ES, Schlütz F, van Geel B. NPP-ID: Non-Pollen Palynomorph Image Database as a research and educational platform. Vegetation History and Archaeobotany 2022; 31: 323-328.

Siemensma FJ. Microworld, world of amoeboid organisms. World-wide electronic publication, Kortenhoef, the Netherlands. https://www.arcella.nl 2022.

Sillasoo U, Väliranta M, Tuittila ES. Fire history and vegetation recovery in two raised bogs at the Baltic Sea. Journal of Vegetation Science 2011; 22: 1084-1093.

Sim TG, Swindles GT, Morris PJ, Gałka M, Mullan D, Galloway JM. Pathways for Ecological Change in Canadian High Arctic Wetlands Under Rapid Twentieth Century Warming. Geophysical Research Letters 2019; 46: 4726-4737.

Słowiński M, Błaszkiewicz M, Brauer A, Noryśkiewicz B, Ott F, Tyszkowski S. The role of melting dead ice on landscape transformation in the early Holocene in Tuchola Pinewoods, North Poland. Quaternary International 2015; 388: 64-75.

Słowiński M, Lamentowicz M, Łuców D, Barabach J, Brykała D, Tyszkowski S, et al. Paleoecological and historical data as an important tool in ecosystem management. Journal of Environmental Management 2019; 236: 755-768.

Sothe C, Gonsamo A, Arabian J, Kurz WA, Finkelstein SA, Snider J. Large soil carbon storage in terrestrial ecosystems of Canada. Global Biogeochemical Cycles 2022; 36: e2021GB007213.

Stevenson JA, Millington SC, Beckett FM, Swindles GT, Thordarson T. Big grains go far: understanding the discrepancy between tephrochronology and satellite infrared measurements of volcanic ash. Atmos. Meas. Tech. 2015; 8: 2069-2091.

Stivrins N, Kalnina L, Veski S, Zeimule S. Local and regional Holocene vegetation dynamics at two sites in eastern Latvia. Boreal Environment Research 2014; 19: 310-322.

Swindles GT, Morris PJ, Mullan DJ, Payne RJ, Roland TP, Amesbury MJ, et al. Widespread drying of European peatlands in recent centuries. Nature Geoscience 2019; 12: 922-928.

Tanneberger F, Moen A, Barthelmes A, Lewis E, Miles L, Sirin A, et al. Mires in Europe—Regional Diversity, Condition and Protection. Diversity 2021; 13: 381.

Tinner W, Hu FS. Size parameters, size-class distribution and area-number relationship of microscopic charcoal: relevance for fire reconstruction. The Holocene 2003; 13: 499-505.

Tobolski K. Przewodnik do oznaczania torfów i osadów jeziornych: PWN, Warszawa, 2000.

Trachsel M, Telford RJ. All age–depth models are wrong, but are getting better. The Holocene 2016; 0: 0959683616675939.

Turetsky MR, Benscoter B, Page S, Rein G, van der Werf GR, Watts A. Global vulnerability of peatlands to fire and carbon loss. Nature Geosci 2015; 8: 11-14.

Turner TE, Swindles GT. Ecology of Testate Amoebae in Moorland with a Complex Fire History: Implications for Ecosystem Monitoring and Sustainable Land Management. Protist 2012; 163: 844-855.

Turner TE, Swindles GT, Roucoux KH. Late Holocene ecohydrological and carbon dynamics of a UK raised bog: impact of human activity and climate change. Quaternary Science Reviews 2014; 84: 65-85.

van Bellen S, Mauquoy D, Hughes PD, Roland TP, Daley TJ, Loader NJ, et al. Late-Holocene climate dynamics recorded in the peat bogs of Tierra del Fuego, South America. The Holocene 2016; 26: 489-501.

van de Flierdt T, Griffiths AM, Lambelet M, Little SH, Stichel T, Wilson DJ. Neodymium in the oceans: a global database, a regional comparison and implications for palaeoceanographic research. Philosophical Transactions of the Royal Society A: Mathematical, Physical and Engineering Sciences 2016; 374: 20150293.

Vanneste H, De Vleeschouwer F, Bertrand S, Martínez-Cortizas A, Vanderstraeten A, Mattielli N, et al. Elevated dust deposition in Tierra del Fuego (Chile) resulting from Neoglacial Darwin Cordillera glacier fluctuations. Journal of Quaternary Science 2016; 31: 713-722.

Vanneste H, De Vleeschouwer F, Martínez-Cortizas A, von Scheffer C, Piotrowska N, Coronato A, et al. Late-glacial elevated dust deposition linked to westerly wind shifts in southern South America. Scientific Reports 2015; 5: 11670.

Varga G. Changing nature of Saharan dust deposition in the Carpathian Basin (Central Europe): 40 years of identified North African dust events (1979–2018). Environment International 2020; 139: 105712.

Watson EJ, Kołaczek P, Słowiński M, Swindles GT, Marcisz K, Gałka M, et al. First discovery of Holocene Alaskan and Icelandic tephra in Polish peatlands. Journal of Quaternary Science 2017; 32: 457-462.

Watson EJ, Swindles GT, Stevenson JA, Savov IP, Lawson IT. The transport of Icelandic volcanic ash: Insights from northern European cryptotephra records. J. Geophys. Res. Solid Earth 2016; 121: 7177–7192.

White WM, Hofmann AW. Sr and Nd isotope geochemistry of oceanic basalts and mantle evolution. Nature 1982; 296: 821-825.
Whitlock C, Larsen C. Charcoal as a fire proxy. Tracking environmental change using lake sediments. Terrestrial, algal, and siliceous indicators. J. P. Smol, H. J. B. Birks, and W. M. Last, Eds. 3, Dordrecht: Kluwer, 2001, pp. 75-97.
Witze A. The Arctic is burning like never before — and that's bad news for climate change. Nature 2020; 585: 336-337.
Zhang H, Väliranta M, Piilo S, Amesbury MJ, Aquino-López MA, Roland TP, et al. Decreased carbon accumulation feedback driven by climate-induced drying of two southern boreal bogs over recent centuries. Global Change Biology 2020; 26: 2435-2448.

**Table 1**. Results of radiocarbon dating of charcoal sampled from peat from Stawek bog. The radiocarbon dates were calibrated using the IntCal20 calibration curve (Reimer et al., 2020).

| Depth [cm] | Laboratory code | $^{14}$C date [yr. $^{14}$C BP] | Calibrated age [yr. cal. CE] (95.4 % confidence interval) | Material dated |
|---|---|---|---|---|
| 90-91 | Poz-127366 | 320 ± 30 | 1484-1644 (95.4 %) | charcoal |
| 95-96 | Poz-127367 | 565 ± 30 | 1308-1363 (53.7 %)<br>1386-1425 (41.8 %) | charcoal |
| 100-101 | Poz-127368 | 880 ± 30 | 1045-1085 (16.9 %)<br>1093-1105 (1.5 %)<br>1121-1228 (77 %) | charcoal |
| 105-106 | Poz-127572 | 1135 ± 30 | 774-787 (3.9 %)<br>830-855 (5.5 %)<br>873-993 (86.1 %) | charcoal |
| 109-110 | Poz-127369 | 1885 ± 30 | 78-101 (7.1 %)<br>107-234 (88.3 %) | charcoal |

**Table 2**. Reference $\varepsilon_{Nd}$ values measured in surface samples taken from the studied peatlands and their surrounding (Głęboczek – Gł; Stawek – pBS).

| Sample code | Sampling spot, material | $^{143}$Nd/$^{144}$Nd ($t$=0) | $\varepsilon_{Nd}$ ($t$=0) |
|---|---|---|---|
| GŁ2 | slope 1, soil | 0.511787 ±10 | −16.6 |

| | | | |
|---|---|---|---|
| GŁ3 | slope 2, soil | 0.511733 ±10 | −17.7 |
| GŁ4 | peatland, *Sphagnum* | 0.511922 ± 11 | −14.0 |
| GŁ5 | peatland, *Sphagnum* | 0.511928 ± 10 | −13.8 |
| pBS1 | peatland, *Sphagnum* | 0.511867 ± 10 | −15.0 |
| pBS2 | peatland, *Sphagnum* | 0.511843 ± 13 | −15.5 |
| pBS3 | peatland, *Sphagnum* | 0.511899 ±10 | −14.4 |
| pBS4 | slope W, soil | 0.511282 ± 10 | −26.5 |
| pBS5 | slope E, soil | 0.511776 ± 13 | −16.8 |

**Figure 1**

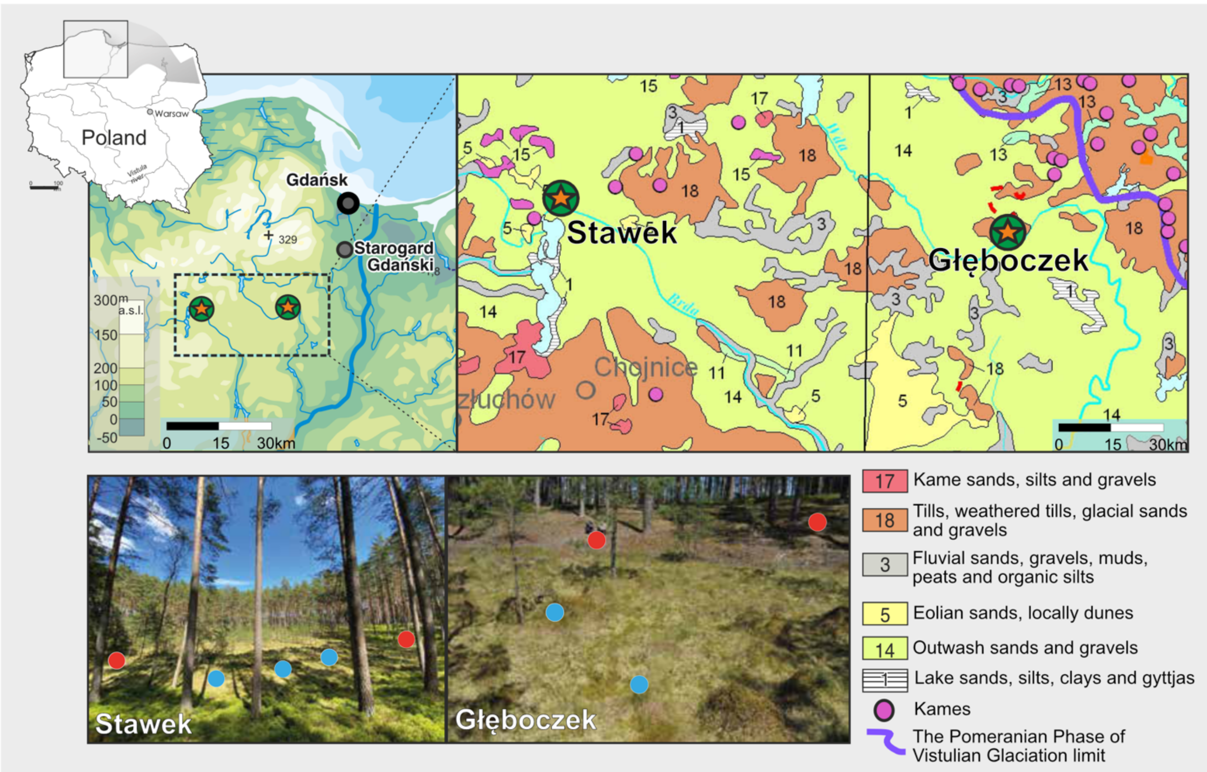


**Figure 2**

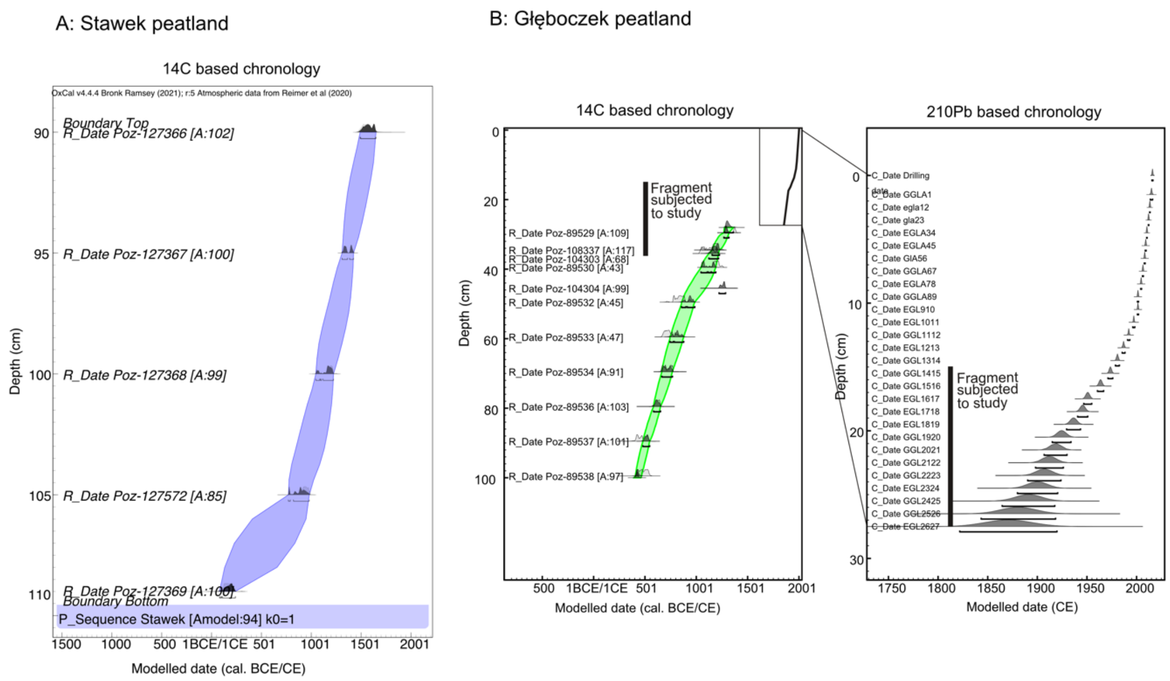
A: Stawek peatland
14C based chronology
OxCal v4.4.4 Bronk Ramsey (2021); r:5 Atmospheric data from Reimer et al (2020)
Boundary Top
R_Date Poz-127366 [A:102]
R_Date Poz-127367 [A:100]
R_Date Poz-127368 [A:99]
R_Date Poz-127572 [A:85]
R_Date Poz-127369 [A:100]
Boundary Bottom
P_Sequence Stawek [Amodel:94] k0=1
Depth (cm)
Modelled date (cal. BCE/CE)
B: Głęboczek peatland
14C based chronology
Fragment subjected to study
R_Date Poz-89529 [A:109]
R_Date Poz-108337 [A:117]
R_Date Poz-104303 [A:68]
R_Date Poz-89530 [A:43]
R_Date Poz-104304 [A:99]
R_Date Poz-89532 [A:45]
R_Date Poz-89533 [A:47]
R_Date Poz-89534 [A:91]
R_Date Poz-89536 [A:103]
R_Date Poz-89537 [A:101]
R_Date Poz-89538 [A:97]
Depth (cm)
Modelled date (cal. BCE/CE)
210Pb based chronology
Fragment subjected to study
Depth (cm)
Modelled date (CE)

**Figure 3**

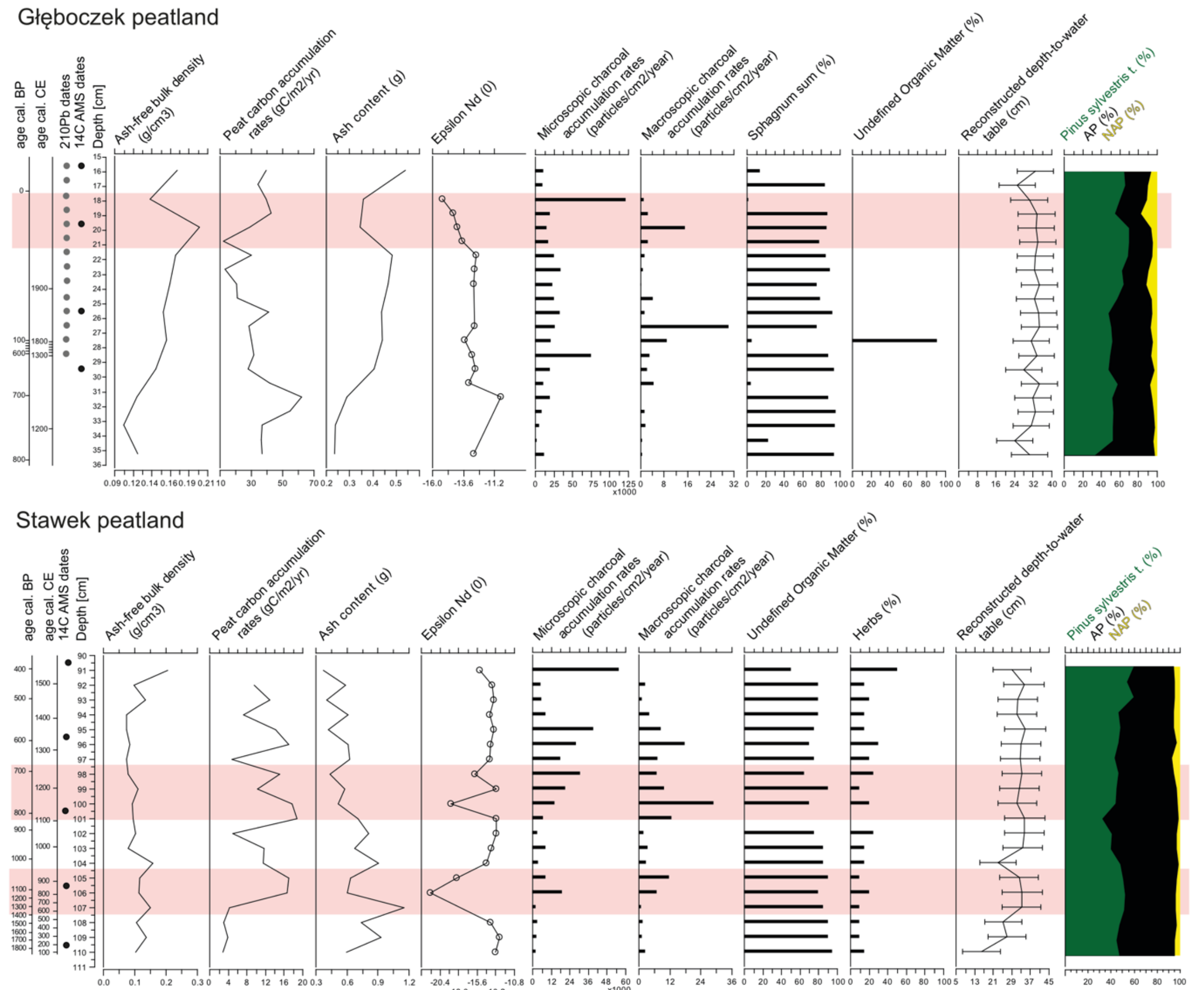
Głęboczek peatland
age cal. BP
age cal. CE
210Pb dates
14C AMS dates
Depth [cm]
Ash-free bulk density (g/cm3)
Peat carbon accumulation rates (gC/m2/yr)
Ash content (g)
Epsilon Nd (0)
Microscopic charcoal accumulation rates (particles/cm2/year)
Macroscopic charcoal accumulation rates (particles/cm2/year)
Sphagnum sum (%)
Undefined Organic Matter (%)
Reconstructed depth-to-water table (cm)
Pinus sylvestris t. (%)
AP (%)
NAP (%)
Stawek peatland
age cal. BP
age cal. CE
14C AMS dates
Depth [cm]
Ash-free bulk density (g/cm3)
Peat carbon accumulation rates (gC/m2/yr)
Ash content (g)
Epsilon Nd (0)
Microscopic charcoal accumulation rates (particles/cm2/year)
Macroscopic charcoal accumulation rates (particles/cm2/year)
Undefined Organic Matter (%)
Herbs (%)
Reconstructed depth-to-water table (cm)
Pinus sylvestris t. (%)
AP (%)
NAP (%)

**Figure 4**

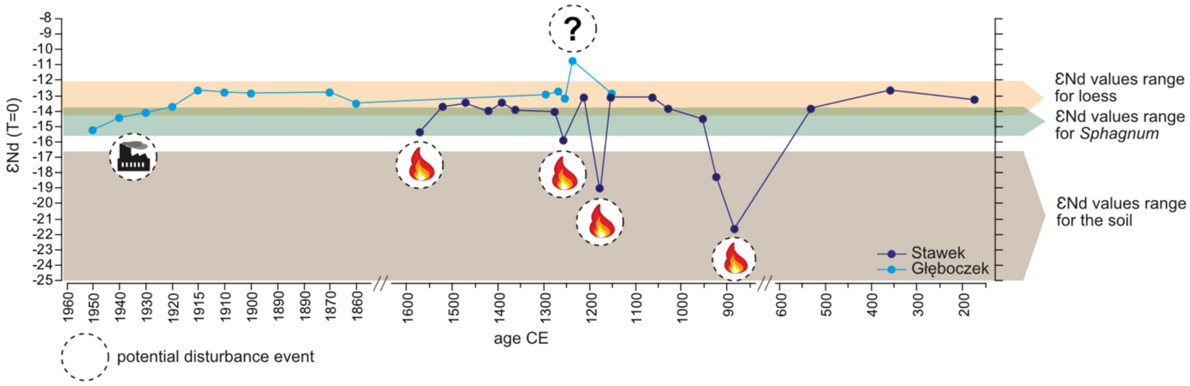

?
εNd values range for loess
εNd values range for *Sphagnum*
εNd values range for the soil
Stawek
Głęboczek
εNd (T=0)
-8
-9
-10
-11
-12
-13
-14
-15
-16
-17
-18
-19
-20
-21
-22
-23
-24
-25
1960
1950
1940
1930
1920
1915
1910
1900
1890
1890
1870
1860
1600
1500
1400
1300
1200
1100
1000
900
600
500
400
300
200
age CE
potential disturbance event